RESEARCH ARTICLE

3D Killer Turn Angle in Transtibial Posterior Cruciate Ligament Reconstruction Is Determined by the Graft Turning Angle both in the Sagittal and Coronal Planes

Gengxin Jia, MD[1,2#], Yuchen Tang, MD[1,2#], Zhongcheng Liu, MD[1,2#], Bo Peng, MD[1,2], Lijun Da, MM[3], Jun Yang, MB[1,2], Xiaolong Liu, MD[1,2], Ming Ma, MD[1,2], Hua Han, MD, PhD[1,2], Meng Wu, MD[1,2], Bin Geng, MD, PhD[1,2], Yayi Xia, MD, PhD[1,2], Yuanjun Teng, MD, PhD[1,2]

[1]*Department of Orthopaedics, Lanzhou University Second Hospital and* [2]*Orthopaedics Key Laboratory of Gansu Province, Lanzhou University Second Hospital, Lanzhou University, Lanzhou and* [3]*Department of Oncology, Lanzhou University Second Hospital, Lanzhou University, Lanzhou City, People's Republic of China*

Objective: During the transtibial posterior cruciate ligament (PCL) reconstruction, surgeons commonly pay more attention to the graft turning angle in the sagittal plane (GASP), but the graft turning angle in the coronal plane (GACP) is always neglected. This study hypothesized that the three-dimensional (3D) killer turn angle was determined by both the GASP and GACP, and aimed to quantitively analyze the effects of the GASP and GACP on the 3D killer turn angle.

Methods: This was an *in-vitro* computer simulation study of transtibial PCL reconstruction using 3D knee models. Patients with knee injuries who were CT scanned were selected from the CT database (April 2019 to January 2021) at a local hospital for reviewing. A total of 60 3D knees were simulated based on the knees' CT data. The femoral and tibial PCL attachment were located on the 3D knee model using the Rhinoceros software. The tibial tunnels were simulated based on different GASP and GACP. The effects of the GASP and GACP on the 3D killer turn angle were quantitatively analyzed. One-way analysis of variance was used to compare the outcomes in different groups. The regression analysis was performed to identify variables of the GASP and GACP which significantly affected 3D killer turn angle.

Results: The 3D killer turn angle showed a significant proportional relationship not only with the GASP ($r^2 > 0.868$, $P < 0.001$), but also with the GACP ($r^2 > 0.467$, $P < 0.001$). Every 10° change of the GACP caused 2.8° to 4.4° change of the 3D killer turn angle, whereas every 10° change of the GASP caused 6.4° to 9.2° change of the 3D killer turn angle.

Conclusions: The 3D killer turn angle was significantly affected by both the GASP and GACP. During the transtibial PCL reconstruction, the proximal anterolateral tibial tunnel approach could increase the 3D killer turn angle more obviously compared with the most distal anteromedial tibial tunnel approach. To minimize the killer turn effect, both the GASP and GACP were required to be considered to increase.

Key words: Graft turning angle; Killer turn; Tibial tunnel approach; Transtibial posterior cruciate ligament reconstruction

Address for correspondence: Yayi Xia and Yuanjun Teng, Department of Orthopaedics, Lanzhou University Second Hospital, No. 82 Cuiyingmen, Chengguan District, Lanzhou City, Gansu, 730030, China. Email: xiayayilzu@126.com and tengyj06@126.com
[#]Gengxin Jia, Yuchen Tang, and Zhongcheng Liu contributed to the work equally and should be regarded as co-first authors.
Received 13 February 2022; accepted 18 June 2022

Orthopaedic Surgery 2022;14:2298–2306 • DOI: 10.1111/os.13411

Introduction

Arthroscopic reconstruction of posterior cruciate ligament (PCL) using transtibial technique is one of the most common surgical procedures to restore the stability of knee joint after PCL injury.[1,2] However, a number of patients have shown unsatisfactory clinical outcomes after the PCL reconstruction, and the required surgical revision rate has reached 26%.[3,4] One of the important reasons associated with the unforeseen postoperative outcomes is the unavoidable abrasion on the graft caused by the "killer turn," which is a sharp angle created by the graft and tibial tunnel at the intraarticular aperture of the tunnel.[3,5,6]

In clinical practice, killer turn is commonly deemed as the graft turning angle in sagittal plane (GASP). Surgeons prefer to increase the GASP to mitigate the graft abrasion of the transtibial PCL reconstruction.[7–9] Nevertheless, the real killer turn angle is the graft angulation in three-dimensional (3D) space. Theoretically, the 3D killer turn angle will be varied when the graft turning angle is changed in the sagittal and coronal planes. Consequently, similar to the GASP, the graft turning angle in coronal plane (GACP) might also be a critical factor affecting the 3D killer turn angle (Fig. 1). However, to date, the effects of the GASP and GACP on the 3D killer turn angle remain unclear.

Although previous studies have used cadaveric and biomechanical models to evaluate the killer turn angle, few studies quantitively analyzed this angle.[7] Due to the limitations of the cadaveric and biomechanical models, the effect of the varied tibial tunnel approach on the 3D killer turn angle is often not accurately analyzed.[10] Fortunately, a novel method of the 3D knee model establishes an *in-vitro* virtual simulation technique, which provides great advantages in precise quantitative analysis and credible repeatability.[11–13] Based on the 3D knee model, the location of the PCL attachment could be precisely located,[14] the tibial tunnel could be monitored in real time, and the 3D killer turn angle, GASP and GACP could be accurately measured and analyzed.

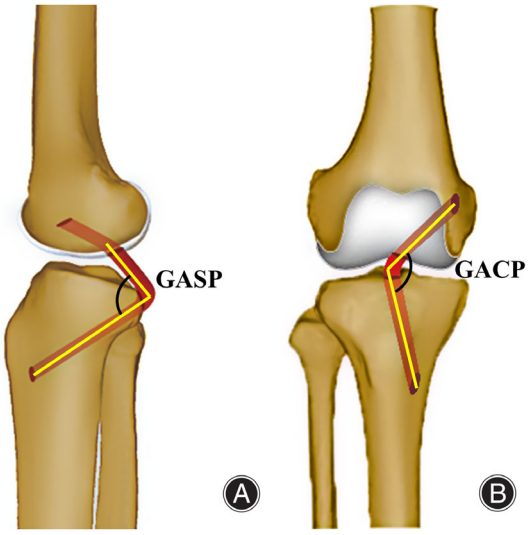

Fig. 1 Schematic of the graft angulation in the sagittal plane and the coronal plane. (A) The graft angulation in the sagittal plane; (B) The graft angulation in the coronal plane

During the transtibial PCL reconstruction, the GASP and GACP are determined by the placement of the tibial tunnel. Increasing the angle between the tibial tunnel and tibial plateau is correlated with a greater GASP, and using the anterolateral tibial tunnel approach is correlated with a greater GACP. Both the surgical procedures to place the tibial tunnel are undoubtedly affecting the 3D killer turn angle.[7,15] Therefore, knowing how the GASP and GACP affects the 3D killer turn angle could help in exploring the optimal tibial tunnel approach. Surgeons could adjust the tibial tunnel entry point based on the effects of the GASP and GACP on the 3D killer turn to reduce the killer turn effect maximally. In this study, the purposes were to: (i) analyze the effects of the GASP and GACP on the 3D killer turn angle in the transtibial PCL reconstruction; and (ii) explore the optimal tibial tunnel approach that could maximize the 3D killer turn angle. The hypothesis of the study was that the 3D killer turn angle was determined by both the GASP and GACP, and surgeons could adjust the GASP and GACP to minimize the killer turn effect.

Methods

This is a computer simulation study of transtibial PCL reconstruction using 3D knee models. This study was approved by the regional ethics committee (2021A-169). Three hundred thirty six patients who were CT scanned for knee injuries over a two-year period from 2019 to 2021 in local hospital were retrospectively reviewed. The inclusion criteria in this study were as follows: (i) patients with knee injury; (ii) age of patients ranged from 18 to 60 years; (iii) the CT images with ultrahigh resolution which could be used for accurate 3D model simulation and clearly identified the tibial PCL attachment; and (iv) Kellgren–Lawrence grade less than 1;[5] Exclusion criteria were: CT images showed with morphological abnormalities or dysplasia, fractures, history of knee surgery and soft tissue injuries. Lastly, 60 knee joints' CT images were included in this study. Table 1 shows the patient demographic data.

Establishment of 3D *Knee Joint Model*

All included patients underwent routine clinical knee CT performed on a 64-multidetector-row CT (SOMATOM Sensation, Siemens AG, Munich, Germany). Scanning parameters included a gantry rotation speed of 1.00 s/rotation, 0.625 mm collimation width × 12 detectors, a CT pitch factor of 0.90, and a field of view of 25–30 cm. The CT dose index (CTDI) volume was 20.9 mGy. The CT images were imported in Digital Imaging and Communications in Medicine (DICOM) format. The DICOM images were processed in MIMICS software (Materialise, Leuven, Belgium) to obtain the 3D model of the knee joint, and the coordinate

data was imported to the Rhinoceros 3D modeling software (Rhino 7, Robert McNeel and Associates for Windows, Washington DC, USA) for measurements of spatial images.

Location of the Femoral and Tibial PCL *Attachments*

In this study, the midpoint of the anterolateral bundle (ALB) and posteromedial bundle (PMB) on the medial femoral condyle was defined as the center of the femoral PCL attachment to simplify the measurement. By rotating the knee model on 3D perspective to strictly overlap the medial and lateral femoral condyles on Rhino software, the true lateral and anteroposterior (AP) view of the femur was acquired (Fig. 2A,B). Line A intersecting with the intercondylar apex and perpendicular to the distal margins of the femoral condyles (distal condyle line) was drawn at the AP view (Fig. 2A). Using line A to cut the femur at the AP view, the femoral sagittal section was obtained. Subsequently, the Blumensaat's line could be drawn on the femoral sagittal section at the lateral view (Fig. 2B).

By referring to the study of Johannsen *et al.*[16] (the ALB center and PMB center were respectively located 14.1 mm and 15.8 mm superior to the distal condyle line, and respectively located 4.7 mm and 10.7 mm posteroinferior from the Blumensaat line), the projection of the center point of the femoral PCL attachment was drawn 15 cm superior to the distal condyle line and 7.7 cm posteroinferior to the Blumensaat's line on the lateral view. The real femoral PCL point was then obtained by using the projection function of the Rhinoceros software (Fig. 2C).

The grayscale value of the CT image was manually adjusted to show the tibial PCL attachment clearly, where the site was widest and inclusive on the sagittal CT image. A point on the tibial attachment center was then marked. A 3D

TABLE 1 Patient demographic data

Parameter	Value [mean ± SD (range)]
Number	60
Sex (male/female)	17:43
Age (years)	35.5 ± 7.1 (18–51)
Height (m)	1.65 ± 0.1 (1.44–1.89)
Weight (kg)	65.7 ± 13.3 (39.9–94.2)
BMI (kg/m^2)	24.2 ± 3.9 (15.9–33)

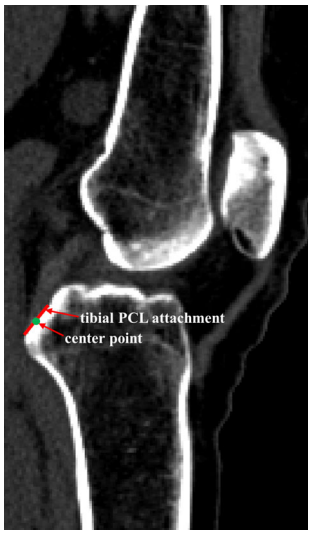

Fig. 3 The center point of the PCL attachment was determined on the sagittal-plane of the knee's CT image

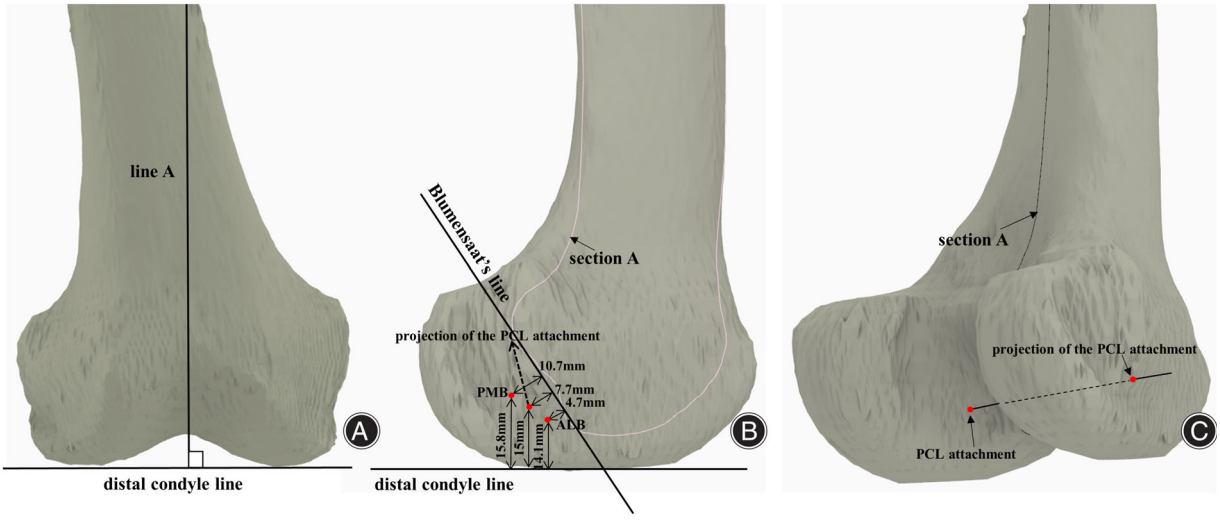

Fig. 2 The method to obtain the femoral PCL attachment site. (A) Line A perpendicular to the tangent line of the distal margins was used to cut the femur in the AP view to obtain the section A; (B) Based on the section A, the Blumensaat's line could be drawn on the lateral view of the femur. (C) The real femoral PCL point was then obtained by using the projection function of the Rhinoceros software

coordinate of the tibial attachment center point was acquired on the Mimics software and imported in to the Rhinoceros 3D modeling software. The exit point of the tibial tunnel in transtibial PCL reconstruction was then obtained (Fig. 3).

Simulation of Tibial Tunnels for Transtibial PCL *Reconstruction*

In this study, the referenced plane for simulating the tibial tunnels was the medial tibial plateau plane. The steps to create the referenced plane were as follows. First, using a best-fit circle tangent to the cortical edge of medial tibial plateau to produce three tangent points (the peak point of the anterior side of the medial tibial plateau; the most medial point of the tibial plateau; the peak point on the posterior side of the medial tibial plateau). Second, these three points were imported into the Rhinoceros 3D modeling software to generate the medial tibial plateau plane (Fig. 4A).[17,18] Third, the tibial plateau plane was translated inferior to intersect with the exit point of the tibial tunnel, and this plane was defined as plane A. In this way, the angle of tibial tunnel relative to plane A and tibial plateau plane was equally when simulate tibial tunnels (Fig. 4B).

In this study, the five tibial tunnels at an angle of 40° relative to the plane A in sagittal plane were simulated. The entire processes were as follows. First, through the exit point of the tibial tunnel, a straight line at an angle of 40° relative to the plane A was drawn in the lateral view. Using this line to cut the tibia in the lateral view, an oblique tibial section was then created (the angle between the oblique tibial section and plane A was 40°) (Fig. 4B,E). Second, the most anterior point of the tibial crest on the oblique tibial section and the tibial tunnel exit point was connected by 0° line (the 0° line was defined as the center line of the tibial tunnel and the entry point was located on the most anterior part of the tibial crest (Fig. 4E). Third, four entry points of the tibial tunnel were marked on the edge of the oblique

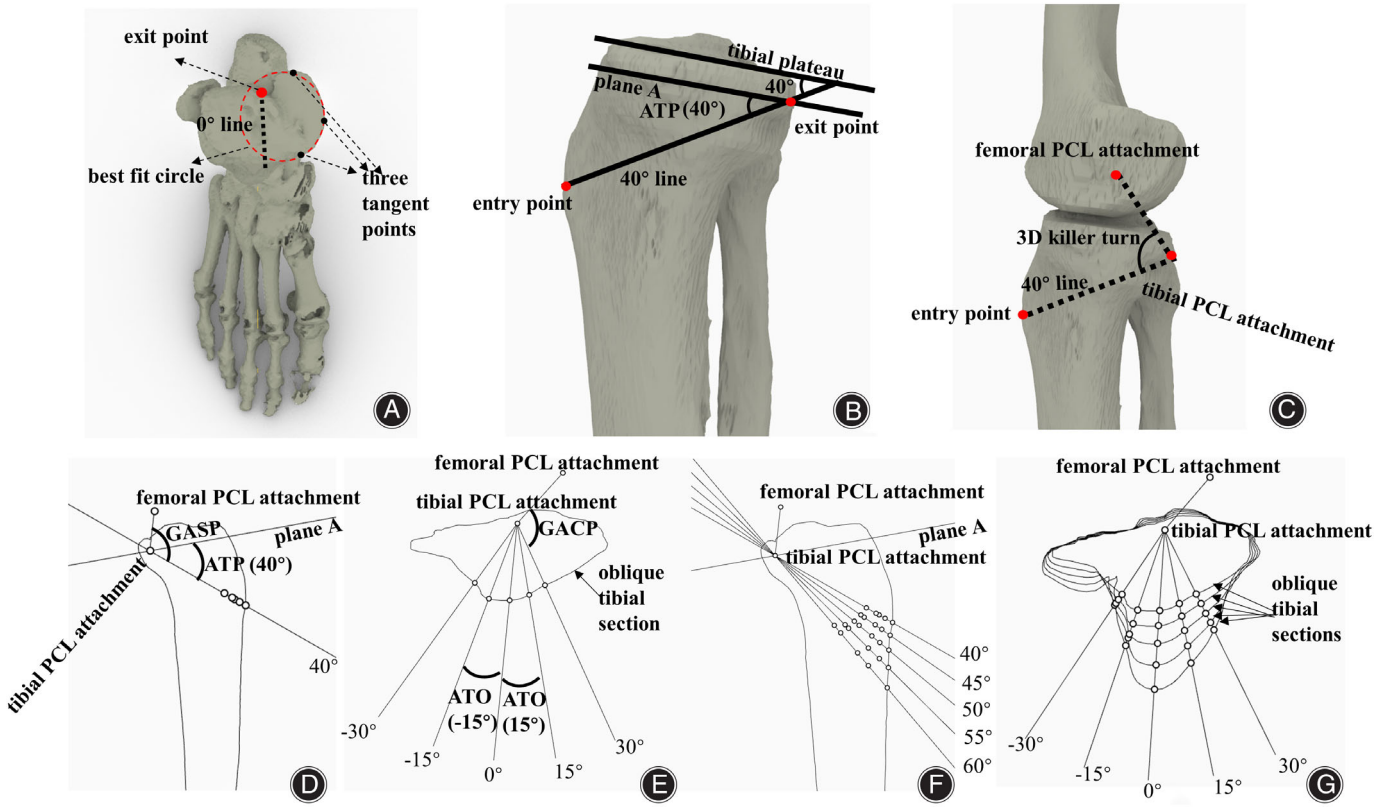

Fig. 4 The method to measure the GASP, GACP and 3D killer turn angle (right knee). (A) 0° line was used to cut the tibia on the axial view to obtain the sagittal section of the tibia. Tibial plateau plane was created by using the best-fit circle. Three tangent points were the tangent points between the best-fit circle and the medial tibial plateau. (B) 40° line was defined as the center line of the tibial tunnel with the entry point on the most anterior tibial crest, and the line relative to the tibial plateau was 40°. Plane A was crossing the tibial tunnel exit point and paralleling to the tibial plateau. (C) Based on outcome of the Fig. 2, the 3D killer turn angle could be measured by using the Rhinoceros 3D modeling software; (D) The GASP could be measured in the tibial sagittal section. ATP was the angle between the plane A and the tibial tunnel in the sagittal plane. (E) The GACP could be measured in the AP view. The oblique tibial section (in AP view) was obtained by using the 40° line to cut the tibia in the sagittal plane. ATO was the angle between the tibial tunnel and the 0°line in the AP view. (F) and (G) The same method as the (D) and (E) to measure the GASP and GACP of all tibial tunnel approaches

tibial section. From the anteromedial to the anterolateral, the angle of the tibial tunnel center lines between the 0° line were −30°, −15°, 15° and 30° respectively. The angle of these five tibial tunnels relative to plane A was 40° in lateral view (sagittal plane) (Fig. 4D,E). The angle between the tibial tunnel and plane A in the sagittal plane was defined as ATP, the angle between the tibial tunnel and 0° line in the coronal plane was define as ATO (Fig, 4D,E). The above procedures were performed continually to simulate the tibial tunnel center lines when the angle between the tibial tunnels and plane A were 45°, 50°, 55° and 60°, respectively (Fig. 4F,G).

Outcome Measurements

GASPs, GACPs and 3D killer turn angles were measured in this study, respectively. The angle between the center line of the tibial tunnel and the connecting line of the PCL attachment site on the femur and tibia in the sagittal plane was defined as GASP, in the coronal plane was defined as GACP, and in the 3D space was defined as 3D killer turn angle (Fig. 4C–E).

Assessment of Methodological Quality

Two board-certified orthopedic surgeons were trained to undertake the measurements. Observer 1 selected 60 knee joints based on the inclusion criteria from the CT image database and undertook the measurement work. After 1 month, Observer 2 remeasured all the specimens to ensure the inter-observer reliability. If any disagreement existed between the observers, the third author would participate in the discussion until a consensus was reached. Intra-observer reliability was calculated using intraclass correlation coefficient (ICC). ICC < 0.40 was considered poor agreement; 0.4 < ICC < 0.75 was considered fair to good agreement; ICC > 0.75 was considered excellent agreement.[19,20] Intraclass correlation has shown excellent intraindividual agreements in this study, and the coefficients ranged from 0.91 to 0.95.

Statistical Analysis

Based on pre-experiment data, the minimum sample size in this study was 50, which was calculated by the G*Power software (version 3.1.9, Heinrich Heine University, Düsseldorf, Germany) using the F test function (one-way analysis of variance (ANOVA): fixed effects, omnibus, one-way) (effect size = 0.61; 1-β err prob. = 0.9; α = 0.05). All data were processed by SPSS software (version 26.0, IBM, Chicago, IL, USA). The results were presented as an arithmetic mean ± standard deviation. Using ANOVA to compare the outcomes in different groups, $P < 0.05$ was considered statistically significant. In order to explore the optimal tibial tunnel approach, the GraphPad Prism (version 9; GraphPad Software, San Diego, CA, USA) software was used to process the single regression analysis to identify the effects of GASP on the 3D killer turn angle when the GACP was fixed, and

TABLE 2 GASP, GACP and 3D killer turn angle in different tibial tunnel approaches

		Parameter mean standard ± deviation				
Groups		40°	45°	50°	55°	60°
−30°	GASP	95.2 ± 8.1	100.2 ± 8.1	105.2 ± 8.1	110.2 ± 8.1	115.2 ± 8.1
	GACP	114.8 ± 6.1	114.8 ± 6.1	114.8 ± 6.1	114.8 ± 6.1	114.8 ± 6.1
	3D angle	85.6 ± 6.5	88.3 ± 6.4	91 ± 6.4	93.7 ± 6.3	96.2 ± 6.2
t value	GASP *vs.* 3D angle	7.161	8.89	10.646	12.481	14.396
	GACP *vs.* 3D angle	25.088	22.93	20.717	18.552	16.422
−15°	GASP	95.2 ± 8.1	100.2 ± 8.1	105.2 ± 8.1	110.2 ± 8.1	115.2 ± 8.1
	GACP	129.8 ± 6.1	129.8 ± 6.1	129.8 ± 6.1	129.8 ± 5.1	129.8 ± 6.1
	3D angle	90.2 ± 6.7	93.7 ± 6.6	97.2 ± 6.6	100.6 ± 6.5	104 ± 6.5
t value	GASP *vs.* 3D angle	3.714	4.82	5.963	7.153	8.404
	GACP *vs.* 3D angle	33.572	30.752	27.42	25.636	22.353
0°	GASP	95.2 ± 8.1	100.2 ± 8.1	105.2 ± 8.1	110.2 ± 8.1	115.2 ± 8.1
	GACP	144.8 ± 6.1	144.8 ± 6.1	144.8 ± 6.1	144.8 ± 6.1	144.8 ± 6.1
	3D angle	94.4 ± 6.8 *	98.5 ± 6.8 *	102.7 ± 6.8 *	106.8 ± 6.7	110.9 ± 6.7
t value	GASP *vs.* 3D angle	0.637	1.237	1.855	2.493	3.174
	GACP *vs.* 3D angle	42.341	38.933	35.546	32.132	28.771
15°	GASP	95.2 ± 8.1	100.2 ± 8.1	105.2 ± 8.1	110.2 ± 8.1	115.2 ± 8.1
	GACP	159.8 ± 6.1	159.8 ± 6.1	159.8 ± 6.1	159.8 ± 6.1	159.8 ± 6.1
	3D angle	98.5 ± 6.9	103.3 ± 6.9	108 ± 6.9	112.7 ± 6.9 *	117.3 ± 6.9 *
t value	GASP *vs.* 3D angle	−2.354	−2.183	−1.983	−1.748	−1.485
	GACP *vs.* 3D angle	51.14	47.204	43.329	39.594	35.593
30°	GASP	95.2 ± 8.1	100.2 ± 8.1	105.2 ± 8.1	110.2 ± 8.1	115.2 ± 8.1
	GACP	174.8 ± 6.1	174.8 ± 6.1	174.8 ± 6.1	174.8 ± 6.1	174.8 ± 6.1
	3D angle	102.9 ± 6.9	108.1 ± 6.9	113.2 ± 6.9	118.2 ± 6.9	122.9 ± 7
t value	GASP *vs.* 3D angle	−5.555	−5.706	−5.786	−5.716	−5.555
	GACP *vs.* 3D angle	58.847	55.44	51.302	47.097	43.074

Note: 3D killer turn angle group compared to the GASP group. $p > 0.05$ *; 3D killer turn angle (3D angle).

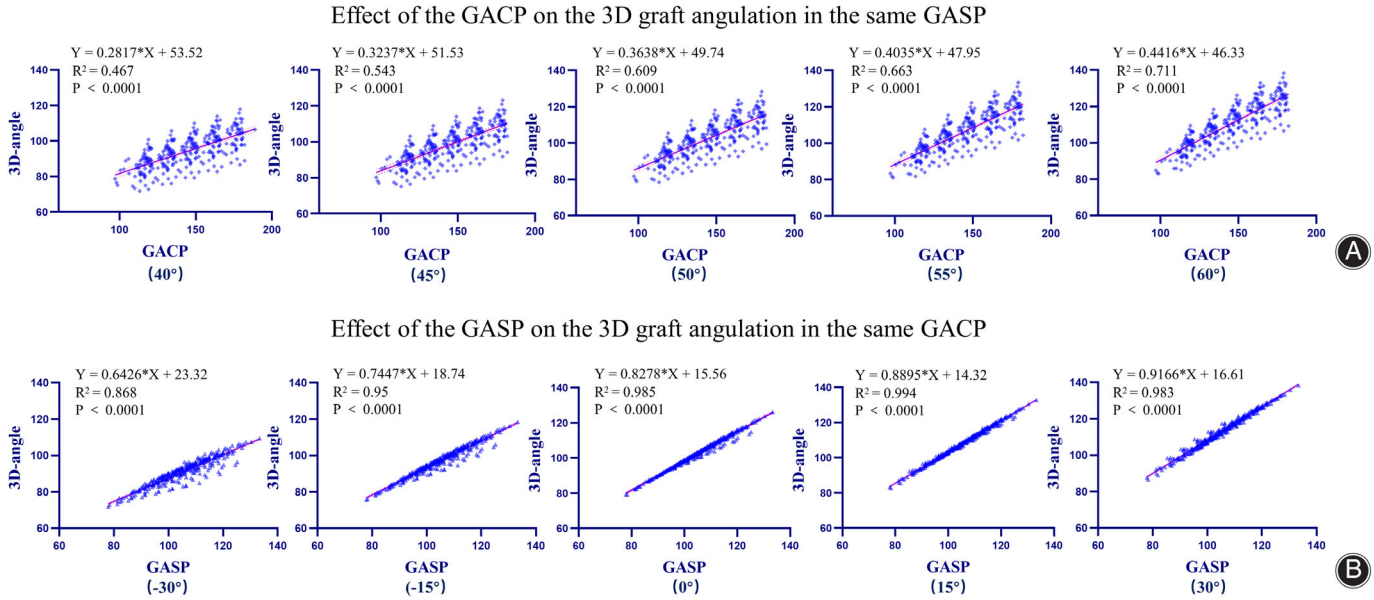

Fig. 5 The linear relationship and the best-fit equations between the 3D killer turn angle and GASP when the GACP was fixed, and the GACP when the GASP was fixed

effects of GACP on the 3D killer turn angle when the GASP was fixed. Goodness of fit was evaluated by coefficients of determination (r^2).

Result

Table 2 shows the mean values were ranged from 85.6° to 122.9° for 3D killer turn angle, ranged from 95.2° to 115.2° for GASP, and ranged from 114.8° to 174.8° for GACP.

The Impact of the GASP *to the* 3D *Killer Turn Angle*

The 3D killer turn angle became significantly less acute as the GASP increased when the GACP was fixed ($P < 0.05$). The 3D killer turn angle was significantly different from the GASP ($P < 0.05$). When the ATO in the coronal plane was −30°, the ATP changed from 40° to 60° in the sagittal plane caused the 3D killer turn angle increase 10.6°. Whereas when the ATO in the coronal plane was 30°, the ATP changed from 40° to 60° in the sagittal plane caused the 3D killer turn angle increase 20° (Table 2).

The Impact of the GACP *to the* 3D *Killer Turn Angle*

The 3D killer turn angle became significantly less acute as the GACP increased when the GASP was fixed ($P < 0.05$). The 3D killer turn angle was significantly different from the GACP ($P < 0.05$). When the ATP in the sagittal plane was 40°, the ATO changed from −30° to 30° in the coronal plane caused the 3D killer turn angle increase 17.4°. Whereas when the ATP in the sagittal plane was 60°, the ATO changed from −30° to 30° in the coronal plane caused the 3D killer turn angle increase 26.7° (Table 2).

Regression Analysis

There was a significant proportional relationship between the GASP and 3D killer turn angle when the GACP was fixed ($r^2 = 0.868$ to 0.994; $P < 0.001$), and between the GACP and 3D killer turn angle when the GASP was fixed ($r^2 = 0.467$ to 0.771; $p < 0.001$). Every 10° change of the GACP caused 2.8°to 4.4° change of the 3D killer turn angle when the GASP was fixed. Every 10° change of the GASP caused 6.4° to 9.2° change of the 3D killer turn angle when the GACP was fixed. According to the Fig, 5A,B, the slope value of the equations was gradually increased (the slope determined amount of change in the y-axis for a 1-unit change in the x-axis), which implied as the GASP became larger, the impact of the GACP to the 3D killer turn angle increased, and as the GACP became larger, the impact of the GASP to the 3D killer turn angle increased.

Discussion

The most important finding of this study is that the 3D killer turn angle is determined by both the GASP and GACP and is significantly different from the GASP and GACP. Therefore, surgeons and researches should not simply deem the GASP or GACP as the 3D killer turn angle. During the PCL reconstruction, both the effects of the GASP and GACP on the 3D killer turn angle should be considered to place the tibial tunnel.

The Effects of the GASP *and* GACP *on the* 3D *Killer Turn Angle*

In this study, the results have showed that not only the GASP should be considered to increase the 3D killer turn

angle during the transtibial PCL reconstruction, but also the GACP. In addition, the impact of the GACP to the 3D killer turn angle would be increased as the GASP became greater, and the impact of the GASP to the 3D killer turn angle would be increased as the GACP became greater. Predictably, increasing the tibial guide angle in the sagittal plane combined with using the anterolateral tibial tunnel approach might reduce the killer turn effect maximumly.

Previous studies have revealed, the killer turn will result compression force concentrated on the graft at the bone-tunnel margin of the proximal tibia. Huang *et al.*[7] have built a mathematic model and found that a sharper graft angulation is correlated with a higher graft compressive force ($F = 2 \times T \times \cos(\theta/2)$, F: compression force; T: graft tension; θ: killer turn angle). Therefore, the variation of the 3D killer turn angle is also correlated to the variation of the compression force on the proximal tibia. In this study, a significant proportional relationship is found between the 3D killer turn angle and the GASP, as well as the GACP. Consequently, it could be concluded that the variation of the compression force on the proximal tibia also have proportional relationship with the variation of the GASP and GACP. In other words, the compression force on the proximal tibia would be decreased as the GASP and GASP increased.

Anterolateral Approach Compared to Anteromedial Approach

A common method to reduce the killer turn effect is to increase the angle between the tibial tunnel and the tibial plateau in sagittal plane during the transtibial PCL reconstruction. However, several studies have reported that this angle could not be increased excessively, for the tibial posterior wall may break and cause risk to the neurovascular bundles in the posterior popliteal fossa.[3,21–23] Recently, Teng *et al.*[10] have reported that the maximum tibial tunnel angle (ATP) for the anteromedial approach in transtibial PCL reconstruction is 58°.

According to the Table 2, the maximum value of the 3D killer turn angle in anteromedial approach could be predicted between 100.6° to 104° when the ATP is 58°. Regarding the anterolateral approach, the 3D killer turn angle is 102.9° when the ATP is 40° and ATO is 30°. However, the recommendations for the tibial guide angle are commonly greater than 40°.[3,24] It could be concluded that the most proximal anterolateral tibial tunnel approach could increase the 3D killer turn angle more obviously compared with the most distal anteromedial tibial tunnel approach. Previously, some studies have suggested that a longer tibial tunnel might aggravate the graft abrasion because of the "bungee effect" and the "windshield wiper effect."[25,26] Also, several studies have reported that the longer tibial tunnel will lead to a less cancellous bone mass in the proximal half of human tibias, and the ability of tendon-bone healing might be also weakened.[27,28] [30,3117,32] Consequently, in terms of providing a slighter graft abrasion and a better tendon-bone healing, using the anterolateral tibial tunnel approach with a proximal entrance is superior to increase the GASP in anteromedial approach. This is important information for surgeons to select the tibial tunnel approach and for researchers to study the optimal tibial tunnel more comprehensively in the future.

The Optimal Tibial Tunnel Approach to Minimize the Killer Turn Effect

Thus far, the studies based on the coronal plane to reduce the killer turn effect are lacking in transtibial PCL reconstruction. Only a few researchers have noticed that the killer turn angle is significantly increased by using the anterolateral approach compared to the anteromedial approach. By studying the knee joint of cadavers and establishing mathematical models, Huang *et al.*[7] reported that the killer turn angle was 114.4° for the anterolateral route and 81.0° for the anteromedial route. Kim *et al.*[29] also proved this by finite element analysis and biomechanical experiments. In the meanwhile, they found that the von Mises stresses (commonly used to evaluate the structural stability) caused by the anterolateral approach were less than caused by the anteromedial tunnel by 33%. However, they have only compared the anterolateral, central, and anteromedial tibial tunnel approach when the drill guide is oriented 45° to the long axis of the tibia. Studies that combined the graft turning angle in the sagittal plane and coronal plane to increase the killer turn angle in the 3D space are rare. Also, the location of the tibial tunnel approach varied in which plane could more significantly impact the "killer turn" in 3D space has not reached a consensus. To our knowledge, few studies have proposed the concept of the graft turning angle in the coronal plane, and few studies have quantitively analyzed the 3D killer turn angle with different tibial tunnel approaches.

According to the results of this study, 3D killer turn angle affected by the GASP is more than the GACP. Nevertheless, the shape of the tibial crest is an inverted triangle. When the tibial tunnel approach changed from anteromedial to the anterolateral, the required angle change in the coronal plane is also found increased on the proximal tibia compared to the distal tibia. The GACP could increase by 30° with the tibial tunnel approach changing from anteromedial to the anterolateral when the ATP is 60° in the sagittal plane (GACP could increase by 60° with the tibial tunnel changing from anteromedial to the anterolateral when the ATP is 40° in the sagittal plane). It could be concluded that the 3D killer turn angle could be increased from 13.3° to 16.9° when the tibial tunnel approach changed from the anteromedial to the anterolateral in the coronal plane. However, with regard to the GASP, every 10° change caused 6.4° to 9.2° change of the 3D killer turn angle when the GACP is fixed. It indicates that changing the tibial tunnel approach from anteromedial to anterolateral could provide a greater 3D killer turn angle compared to only increase the GASP.

In the present study, using the anteromedial tibial tunnel approach does not minimize the killer turn effect even if the GASP is increased to the maximum. Consequently, the

killer turn effect should be further reduced in the anterolateral approach. Also, the 3D killer turn angle is found to be significantly increased as the GASP and GACP increased. Therefore, increasing the GASP on the basis of using the anterolateral approach can minimize the killer turn effect. One step further, both the GASP and GACP are required to be enlarged as much as possible.

Limitations

Our study has the following limitations: (i) this is a theoretical study, which needs basic biomechanical experiments to verify the influence by the variation of the GASP and GACP to the compression force on the proximal tibia. (ii) Some simulated tibial tunnel approaches will not be used in clinical practice, but our study just quantitively analyzed and compared the effects of the variation of the GASP and GACP to the 3D killer turn angle. These tibial tunnel approaches could provide an outcome to observe the changes of the relevant parameters. (iii) The tibial PCL attachment site was located by using the sagittal CT image, which might raise concerns about the precision of the method.

Conclusions

The 3D killer turn angle is determined by both the GASP and GACP. During the transtibial PCL reconstruction, the proximal anterolateral tibial tunnel approach could increase the 3D killer turn angle more significant compared with the most distal anteromedial tibial tunnel approach. To minimize the killer turn effect, both the GASP and GACP are required to increase. Future studies need to explore whether maximizing the 3D killer turn angle could improve the surgical prognosis and reduce the revision rate for the transtibial PCL reconstruction.

Acknowledgment

We would like to thank John Smith for his language assistance.

Funding Statement

National Natural Science Foundation of China (82060413/81874017/81960403/82060405); Gansu Province Science Foundation for Youths (21JR1RA154); Innovation Fund for Universities in Gansu Province (2020B-029); Lanzhou Science and Technology Plan Project (2021-1-106); Cuiying Scientific Training Program for Undergraduates of Lanzhou University Second Hospital (CYXZ2021-17/CYXZ2021-25).

Author Contributions

We declare that each author (Gengxin Jia, Yuchen Tang, Zhongcheng Liu，Bo Peng, Lijun Da, Jun Yang, Xiaolong Liu, Ming Ma, Hua Han, Meng Wu, Bin Geng, Yayi Xia and Yuanjun Teng) has participated the following work for this manuscript.

Gengxin Jia, study design, software, data collections, writing, final corrections. Yuchen Tang and Zhongcheng Liu, data collections, data analysis, software. Bo Peng, Lijun Da and Jun Yang, data analysis, writing. Xiaolong Liu and Ming Ma data collections, writing. Hua Han, Meng Wu and Bin Geng, study design, writing, final corrections.

Yayi Xia and Yuanjun Teng, final corrections, final approval of the version to be published.

References

1. Jung M, Song SY, Cha M, Chung HM, Kim YS, Jang SW, et al. Graft bending angle of the reconstructed posterior cruciate ligament gradually decreases as knee flexion increases. Knee Surg Sports Traumatol Arthrosc. 2020;28:2626–33.
2. Gao SG, Jiang W, Lei GH, Xu M, Yu F, Li KH. Effect of posterior cruciate ligament rupture on biomechanical features of the medial femoral condyle. Orthop Surg. 2011;3:205–10.
3. Shin YS, Kim HJ, Lee DH. No clinically important difference in knee scores or instability between transtibial and inlay techniques for PCL reconstruction: a systematic review. Clin Orthop Relat Res. 2017;475:1239–48.
4. Grassi A, Zicaro JP, Costa-Paz M, et al. Good mid-term outcomes and low rates of residual rotatory laxity, complications and failures after revision anterior cruciate ligament reconstruction (ACL) and lateral extra-articular tenodesis (LET). Knee Surg Sports Traumatol Arthrosc. 2020;28:418–31.
5. Lee DY, Kim DH, Kim HJ, Ahn HS, Lee TH, Hwang SC. Posterior cruciate ligament reconstruction with transtibial or tibial inlay techniques: a meta-analysis of biomechanical and clinical outcomes. Am J Sports Med. 2018;46:2789–97.
6. Weiss WM. Editorial commentary: posterior cruciate ligament femoral techniques: the "critical corner" is just not as exciting as the "killer turn". Art Ther. 2019;35:1195–6.
7. Huang T-W, Wang C-J, Weng L-H, Chan Y-S. Reducing the "killer turn" in posterior cruciate ligament reconstruction. Arthroscopy. 2003;19:712–6.
8. Song EK, Park HW, Ahn YS, Seon JK. Transtibial versus tibial inlay techniques for posterior cruciate ligament reconstruction: long-term follow-up study. Am J Sports Med. 2014;42:2964–71.
9. Bedi A, Musahl V, Cowan JB. Management of posterior cruciate ligament injuries: an evidence-based review. J Am Acad Orthop Surg. 2016;24:277–89.
10. Teng Y, Da L, Jia G, et al. What is the maximum tibial tunnel angle for transtibial PCL reconstruction? A comparison based on virtual radiographs, CT images, and 3D knee models. Clin Orthop Relat Res. 2022;480:918–28. https://doi.org/10.1097/corr.0000000000002111
11. Bhattacharyya R, Ker A, Fogg Q, Spencer SJ, Joseph J. Lateral intercondylar ridge: is it a reliable landmark for femoral ACL insertion?: an anatomical study. Int J Surg. 2018;50:55–9.
12. Qiang M, Chen Y, Zhang K, Li H, Dai H. Effect of sustentaculum screw placement on outcomes of intra-articular calcaneal fracture osteosynthesis: a prospective cohort study using 3D CT. Int J Surg. 2015;19:72–7.
13. Teng Y, Mizu-Uchi H, Xia Y, et al. Axial but not sagittal hinge axis affects posterior tibial slope in medial open-wedge high tibial osteotomy: a 3-dimensional surgical simulation study. Arthroscopy. 2021;37:2191–201.
14. Jeong WS, Yoo YS, Kim DY, Shetty NS, Smolinski P, Logishetty K, et al. An analysis of the posterior cruciate ligament isometric position using an in vivo 3-dimensional computed tomography-based knee joint model. Arthroscopy. 2010;26:1333–9.
15. Kim SJ, Shin JW, Lee CH, Shin HJ, Kim SH, Jeong JH, et al. Biomechanical comparisons of three different tibial tunnel directions in posterior cruciate ligament reconstruction. Arthroscopy. 2005;21:286–93.
16. Johannsen AM, Anderson CJ, Wijdicks CA, Engebretsen L, LaPrade RF. Radiographic landmarks for tunnel positioning in posterior cruciate ligament reconstructions. Am J Sports Med. 2013;41:35–42.
17. Lee YS, Ko TS, Ahn JH, Kang SG, Choi UH, Elazab A, et al. Comparison of tibial tunnel techniques in posterior cruciate ligament reconstruction: C-arm versus anatomic fovea landmark. Arthroscopy. 2016;32:487–92.
18. LaPrade CM, Civitarese DM, Rasmussen MT, LaPrade RF. Emerging updates on the posterior cruciate ligament: a review of the current literature. Am J Sports Med. 2015;43:3077–92.
19. Dean RS, DePhillipo NN, Chahla J, Larson CM, LaPrade RF. Posterior tibial slope measurements using the anatomic axis are significantly increased compared with those that use the mechanical axis. Arthroscopy. 2021;37:243–9.
20. Lertwanich P, Martins CA, Asai S, Ingham SJ, Smolinski P, Fu FH. Anterior cruciate ligament tunnel position measurement reliability on 3-dimensional reconstructed computed tomography. Arthroscopy. 2011;27:391–8.

21. Teng Y, Zhang X, Ma C, Wu H, Li R, Wang H, et al. Evaluation of the permissible maximum angle of the tibial tunnel in transtibial anatomic posterior cruciate ligament reconstruction by computed tomography. Arch Orthop Trauma Surg. 2019;139:547–52.
22. Alentorn-Geli E, Stuart JJ, Choi JH, Toth AP, Moorman CT 3rd, Taylor DC. Posterolateral portal tibial tunnel drilling for posterior cruciate ligament reconstruction: technique and evaluation of safety and tunnel position. Knee Surg Sports Traumatol Arthrosc. 2017;25:2474–80.
23. Nyland J, Fisher B, Brand E, Krupp R, Caborn DN. Osseous deficits after anterior cruciate ligament injury and reconstruction: a systematic literature review with suggestions to improve osseous homeostasis. Arthroscopy. 2010;26: 1248–57.
24. Ahn JH, Bae JH, Lee YS, Choi K, Bae TS, Wang JH. An anatomical and biomechanical comparison of anteromedial and anterolateral approaches for tibial tunnel of posterior cruciate ligament reconstruction: evaluation of the widening effect of the anterolateral approach. Am J Sports Med. 2009;37:1777–83.
25. Höher J, Möller HD, Fu FH. Bone tunnel enlargement after anterior cruciate ligament reconstruction: fact or fiction? Knee Surg Sports Traumatol Arthrosc. 1998;6:231–40.
26. L'Insalata JC, Klatt B, Fu FH, Harner CD. Tunnel expansion following anterior cruciate ligament reconstruction: a comparison of hamstring and patellar tendon autografts. Knee Surg Sports Traumatol Arthrosc. 1997;5:234–8.
27. Zhang X, Teng Y, Yang X, Li R, Ma C, Wang H, et al. Evaluation of the theoretical optimal angle of the tibial tunnel in transtibial anatomic posterior cruciate ligament reconstruction by computed tomography. BMC Musculoskelet Disord. 2018;19:436.
28. Li Y, Chen X, Zhang J, Song G, Li X, Feng H. What role does low bone mineral density play in the "killer turn" effect after transtibial posterior cruciate ligament reconstruction? Orthop Surg. 2016;8:483–9.
29. Kim SJ, Chang JH, Kang YH, Song DH, Park KY. Comparison of the clinical results of three posterior cruciate ligament reconstruction techniques. J Bone Jt Surg, Am. 2009;91:2543–9.